Title

Netload Range Cost Curves for Coordinated Transmission-Distribution Planning Under DER Growth Uncertainty

Journal
IEEE Transactions on Energy Markets Policy and Regulation, 4(1)

ISSN
2771-9626

Authors
Li, Yujia
Córdova, Samuel
Moreira, Alexandre
et al.

Publication Date
2026-03-01

DOI
10.1109/tempr.2025.3638837

Netload Range Cost Curves for Coordinated Transmission-Distribution Planning Under DER Growth Uncertainty

Yujia Li, *Member, IEEE*, Samuel Córdova, *Member, IEEE*, Alexandre Moreira, *Senior Member, IEEE*, and Miguel Heleno, *Senior Member, IEEE*

***Abstract*—The increasing penetration of distributed energy resources (DERs) requires better coordination between transmission and distribution (T&D) planning to ensure system security and cost efficiency. However, misaligned planning horizons, computational burdens, and privacy concerns hinder effective coordination, leading to either underutilized resources caused by overinvestments or reliability risks due to underinvestment. To address this challenge, we introduce netload range cost curves (NRCCs), a novel approach for managing long-term DER growth uncertainty through T&D coordination, while preserving existing data-sharing and regulatory structures. NRCCs provide pairs of (i) peak substation netload guarantees and (ii) corresponding distribution upgrade options and costs, enabling their seamless integration into transmission planning workflows. To compute NRCCs efficiently, we develop a transmission-aware distribution network planning (TADNP), which is subsequently integrated to an iterative computation procedure. These NRCCs are then embedded into an NRCC-informed transmission planning model to enable resource-efficient coordination. We illustrate our proposed approach with a case study based on realistic distribution and transmission systems in the San Francisco Bay Area, California. Our results indicate the possibility of dramatic savings in transmission investments by incorporating the proposed NRCC-integrated T&D coordination framework.**

***Index Terms*—Distributed energy resources (DERs), long-term uncertainty, netload range cost curve (NRCCs), transmission and distribution coordination.**

NOMENCLATURE

Indices

k	Index of NRCC options.
(m, n)	Index of directed distribution line from DN node m to n.
d/t	Index of representative days/time periods.
n	Index of distribution nodes.
r	Index of candidate line upgrade options.
s	Index of scenarios.
i	Index of transmission nodes.

Sets

$\mathcal{K}$	Set of NRCC options.
$\mathcal{D}/\mathcal{T}$	Set of representative days/time periods.
$\mathcal{L}$	Set of lines.
$\mathcal{L}^{\text{c}}$	Set of candidate lines for reinforcement.
$\mathcal{L}^{\text{FH}}$	Set of feeder heads.
$\mathcal{L}^{\text{VR}}$	Set of candidate voltage regulators.
$\mathcal{N}$	Set of distribution nodes.
$\mathcal{N}^{\text{B}}$	Set of candidate storages.
$\mathcal{N}^{\text{sub}}$	Set of substations.
$\mathcal{N}^{\text{TN}}$	Set of transmission nodes.
$\mathcal{S}$	Set of scenarios.
Ω^{P}	Set of line upgrade options.

Constant parameters

$\overline{S}_{mn}^{L,fixed}$	Capacity of line (m, n) not candidate for reinforcement.
$D_{i,d,t,s}^{\text{load},0}$	Baseline demand at transmission bus i.
$\Delta S_{mn}^{\text{FH}}$	Potential upgrade capacity for feeder head (m, n).
$\eta_n^{\text{c}}/\eta_n^{\text{d}}$	Charging/discharging efficiency of storage n.
$\overline{P}_n^{\text{st,c}}/\overline{P}_n^{\text{st,d}}$	Unit power charging/discharging capacity of storage n.
$\overline{S}_{mn}^{\text{FH,fixed}}$	Initial capacity of feeder head transformer (m, n).
ψ	Reactive contribution capacity of storage n.
$\underline{U}_n^{\text{sqr}}/\overline{U}_n^{\text{sqr}}$	Minimum/maximum squared voltage.
$\varphi_{mn}^{\min}/\varphi_{mn}^{\max}$	Minimum/maximum turns ratio of voltage regulator (m, n).
C^{I}	Imbalance cost.
$C_{mn,r}^{\text{L}}$	Unit cost to upgrade line (m, n) for the option r.
C_n^{st}	Annualized investment cost to install storage n.
C_{mn}^{VR}	Annualized investment cost to upgrade line segment (m, n) with a voltage regulator.

Received 25 February 2025; revised 8 July 2025 and 3 October 2025; accepted 19 November 2025. Date of publication 1 December 2025; date of current version 17 March 2026. This work was supported by the U.S. Department of Energy under Contract DE-AC02-05CH11231. Paper no. TEMPR-00045-2025. *(Corresponding author: Alexandre Moreira.)*

Yujia Li, Alexandre Moreira, and Miguel Heleno are with Lawrence Berkeley National Laboratory, Berkeley, CA 94720 USA (e-mail: yujiali@lbl.gov; AMoreira@lbl.gov; MiguelHeleno@lbl.gov).

Samuel Córdova is with the Department of Electrical Engineering, School of Engineering, Faculty of Engineering, Pontificia Universidad Católica de Chile, Santiago 7820436, Chile, and also with the UC Energy Research Center, Pontificia Universidad Católica de Chile, Santiago 7820436, Chile (e-mail: sacordov@uc.cl).

Digital Object Identifier 10.1109/TEMPR.2025.3638837

C_{mn}^{FH}	Annualized investment cost to upgrade the feeder head transformer (m,n).
$P_{n,d,t,s}^{\mathrm{load}}/Q_{n,d,t,s}^{\mathrm{load}}$	Active/reactive power load at bus n
$R_{mn,r}/X_{mn,r}$	Resistance/Reactance associated with upgrade option r of segment (m,n).
T_n^{st}	Duration of the storage n.
u^{ref}	Reference feeder voltage.
w_d	Weight of the representative day d.
$\mathrm{cap}_{mn,r}$	Reinforced capacity of line (m,n) under the option r.
prob_s	Probability of scenario s.
$\Delta\Gamma_k$	Capital cost of NRCC service.
Γ^0	Least-cost feasible budget derived from the scenario-based least-cost model.
Λ^D/Λ^R	Expected peak direct/reverse substation netloads from the deterministic least-cost model.

Decision Variables

$D_{i,d,t,s}^{\mathrm{load},\dagger}$	Realized demand after NRCC service implementation.
$x_{i,k}^{\mathrm{NRCC},\dagger}$	Binary variable indicating the purchase of NRCC service k.
$e_{n,d,t,s}^{\mathrm{st}}$	State of charge of storage n.
$p_{n,d,t,s}^{\mathrm{I},+}/p_{n,d,t,s}^{\mathrm{I},-}$	Active power surplus/deficit at bus n.
$p_{mn,d,t,s}^{\mathrm{L}}/q_{mn,d,t,s}^{\mathrm{L}}$	Active/reactive power flow through (m,n).
$p_{n,d,t,s}^{\mathrm{sub}}/q_{n,d,t,s}^{\mathrm{sub}}$	Active/reactive power from the upstream substation n.
$q_{n,d,t,s}^{\mathrm{I},+}/q_{n,d,t,s}^{\mathrm{I},-}$	Reactive power surplus/deficit at bus n.
$u_{n,d,t,s}^{\mathrm{sqr,mid}}$	Auxiliary variable related to the squared voltage of node n considering a voltage regulator.
$u_{n,d,t,s}^{\mathrm{sqr}}$	Squared voltage at node n.
$x_{mn}^{\mathrm{FH}}/x_{mn}^{\mathrm{VR}}$	Binary variable indicating the upgrade of feeder head (m,n).
$x_{mn,r}^{\mathrm{L}}$	Binary variable indicating a distribution line (m,n) is reinforced with the option r.
x_n^{st}	Continuous variable indicating the installed capacity of storage n.
λ^D/λ^R	Peak direct and reverse substation netloads among all considered scenarios.
$p_{n,d,t,s}^{\mathrm{st,c}}/p_{n,d,t,s}^{\mathrm{st,d}}$	Charging/discharging power of storage n.
$q_{n,d,t,s}^{\mathrm{st}}$	Reactive power of storage n.
$\overline{S}_{mn}^{\mathrm{L}}$	Capacity of asset (m,n) after decision on potential reinforcement.

I. Introduction

The power industry is undergoing a transformative shift toward sustainable electricity production, partially driven by the increasing penetration of distributed energy resources (DERs) in distribution networks. This shift challenges traditional planning frameworks which were designed for more centralized, predictable power systems [1]. Among these challenges, the increasing integration of behind-the-meter renewable energy sources (RESs), such as rooftop photovoltaics (RPVs), stands out due to their inherent variability and uncertain future adoption growth trajectories. These characteristics complicate long-term planning, in which decisions must account for a wide range of possible future scenarios [2]. In this context, distribution system operators (DSOs) are increasingly expected to assume a more proactive role in managing RES uncertainty and leveraging the controllable DERs, such as battery energy storage systems (BESSs). Moreover, proactive DSO management extends beyond the distribution network. DSOs have the potential to significantly influence the planning and operational decisions of upstream transmission system operators (TSOs) and to support deferring costly infrastructure investments. This represents a massive opportunity to achieve critical investment savings and can be accomplished by enabling a tighter coordination between TSOs and DSOs in both the short and long run.

Traditionally, planning decisions for transmission and distribution systems are optimized separately, and, from the transmission side's point of view, distribution systems are simply regarded as fixed load profiles. However, resources connected to the distribution grid already sell energy into wholesale markets and provide services to support grid management [3]. Currently, the technical literature mostly highlights the roles that DSOs can play to facilitate the TSOs in the short to mid-term operational contexts. For instance, a hierarchical coordination scheme is proposed in [4] to assist DSOs for participating in the European energy balancing markets. In addition, the authors in [5] present a two-stage transmission and distribution (T&D) coordination considering day-ahead and real-time congestion management. Moreover, frequency regulation [6], voltage support [7], and participation in the reserve market [8] are also studied in relevant works. Furthermore, the EPRI-facilitated working group identifies information, control and monitoring interactions to address the needs for T&D coordination [9]. The CoordiNet project, funded by the EU's Horizon 2020 projects [10], established various TSO-DSO-consumer coordination schemes to enable short-term flexibility market participation for customers and small market players.

Despite the great deal of aforementioned research dedicated to propose T&D models and market schemes to harness operational flexibility [4], [5], [6], [7], [8], [9], [10], T&D coordinated investment planning process have not been fully addressed and, in practice, still suffer from limited data exchange and often misaligned planning cycles. As a matter of fact, there is no existing mechanisms currently in place to incentivize distribution utilities to reduce their peak netloads at a planning stage [11], despite this being a key concern for TSOs, as it directly impacts transmission-side investments. The absence of such incentives results in suboptimal investment decisions, as transmission planners cannot adjust their reinforcement strategies based on flexible substation-level netload management that DSOs could have implemented. Specifically, T&D coordination in planning faces several critical challenges: (1) managing the long-term growth uncertainty of behind-the-meter RESs during resource investment; (2) designing products and services compatible with current regulatory frameworks; (3) ensuring the replicability of proposed coordination methodology; and (4) attracting resource investments from utilities and stakeholders.

A few relevant works take into account long-term DER growth uncertainty in distribution grid planning models [12], [13], [14], but they do not account for the potential savings that can be achieved through T&D planning coordination. For instance, worst-case peak netload scenarios in distribution systems can propagate upstream, resulting in overly conservative and costly transmission planning investments [15]. While we concentrate on worst-case netload scenarios to focus on investments that ensure operational feasibility, we acknowledge that system reliability (against outages) may also be improved by proactively deploying local resources in the distribution network [16] [17]. For example, instead of large transmission upgrades, targeted placement of BESS and other DSO-managed assets may be able to meet adequacy and reliability needs at a lower cost. The lack of coordination between T&D planning thus leads to resource duplication and inefficient investment strategies. This issue is further exacerbated by the increasing netload uncertainty at the long-term planning stage, driven by the stochastic nature of DER adoption and integration by end-users.

Centralized and decentralized frameworks have been proposed as attempts to address the regulation and computational aspects of T&D coordination. Centralized approaches, on the one hand, require TSOs to aggregate all grid parameters and data to solve a comprehensive, large-scale optimization problem [18]. While these methods can theoretically yield globally optimal solutions, they are often impractical due to conflicts with the independent planning workflows of TSOs and DSOs, as well as regulatory restrictions on data sharing. Decentralized frameworks, on the other hand, aim to overcome these limitations by decomposing the problem into smaller, more manageable subproblems. Techniques such as distributed optimization [19], [20], and game theory-based methods [21] would allow TSOs and DSOs to iteratively solve their respective optimization problems, coordinating through shared variables through boundary bus constraints. However, while decentralized methods can reduce the need for centralized data aggregation, they still require access to commercially sensitive and proprietary data, therefore challenging the current low levels of data exchange and the lack of standardized protocols between planning entities [22]. Moreover, decentralized methods often struggle with convergence issues, particularly when applied to solve mixed-integer programming problems at large scales, thereby limiting their practical applicability [23].

Furthermore, centralized and decentralized methods proposed so far lack a well-defined incentive mechanism to promote collaboration between T&D entities while preserving their independence in the planning process. For instance, the high investment cost of distributed BESSs could be better justified if their value in deferring or avoiding more cost-intensive transmission infrastructure investments were explicitly quantified [24]. Recently, the concept of flexibility-vs-cost curves has gained considerable attention [25], [26], [27]. These curves effectively represent the aggregate flexibility available on the distribution side as seen by the transmission side, facilitating direct and secure interaction between TSOs and DSOs. By providing explicit values for various levels of flexibility, this approach offers a practical tool for managing the short-term variability of RESs. However, its use has so far been confined to operational contexts, leaving the impact of long-term RES growth uncertainty on the substation netload level in the planning stage largely untapped.

To bridge these gaps, we propose a novel methodology for distribution system planning that explicitly accounts for DER growth uncertainty while providing various options for transmission system planners. These options, presented as netload range cost curves (NRCCs), describe substation peak netload conditions achieved through various possible distribution investment plans. The contributions are threefold:

1) Based on a transmission-aware distribution network planning (TADNP) model, we propose the concept of NRCC, a simple and compact representation of distribution-side planning flexibility to be offered to the transmission. The NRCCs provide a "menu" of distribution system investment plans, each associated with specific long-term netloads and associated investment costs. NRCCs effectively manage uncertainty in long-term DER growth while being amenable to be seamlessly integrated within the planning workflow of TSOs.
2) By leveraging NRCCs computed by DSOs, we introduce the NRCC-informed transmission planning model that enables effective T&D coordination. In this way, the independence of transmission and distribution planning is preserved, which makes NRCCs compatible with existing regulatory frameworks and planning practices.
3) We demonstrate that our proposed NRCC framework can lead to millions of dollars in savings related to avoided transmission reinforcements. These savings can potentially translate directly into an actionable, market-compatible incentive for distribution utilities to invest in non-wires alternatives (NWAs) such as BESS installations. We quantify these benefits via thorough experiments utilizing realistic transmission-distribution networks located in the San Francisco Bay Area.

The rest of the paper is organized as follows: Section II describes the NRCC-integrated T&D coordination architecture and compact planning models for NRCC calculation and utilization. Section III presents the detailed mathematical formulation and solution process for the planning model. Numerical results are presented and analyzed in Section IV. Section V concludes the paper.

II. NRCC and the T&D Coordinated Planning Process: Concept and Models

In this section, we present the concept of NRCC and its use in T&D coordinated planning. We also present the compact formulations for the models to generate the NRCCs on the distribution side, and to incorporate the generated NRCCs into the transmission planning process.

A. T&D Planning Process With NRCC

The NRCC expresses future peak load reduction options at the T&D boundary nodes that can be achieved via realistic

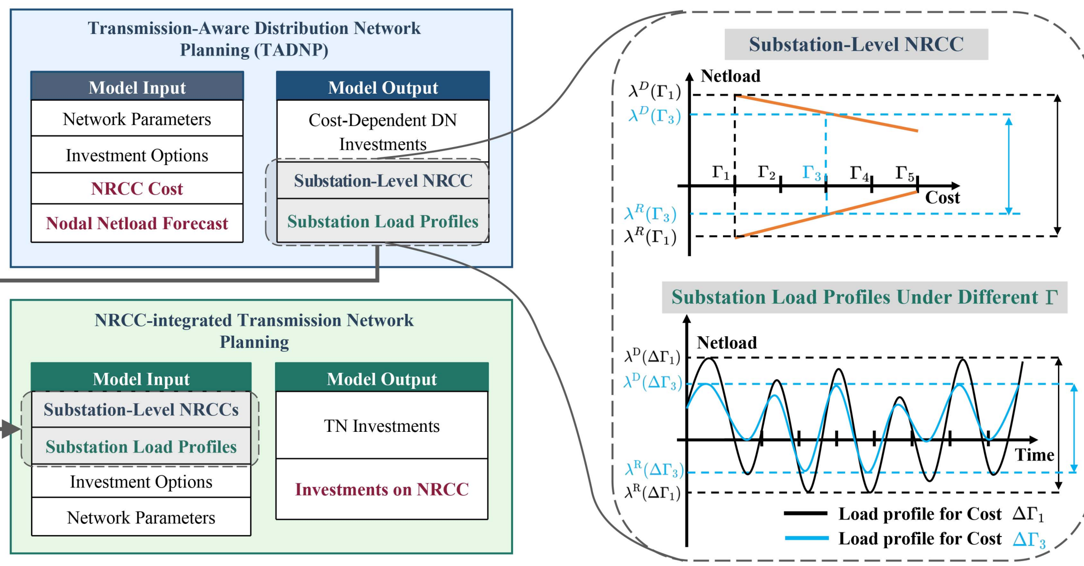

Fig. 1. T&D planning process with NRCCs.

distribution grid investments. Fig. 1 illustrates the use of a substation-level NRCC in the coordinated planning process between a DSO and a TSO. In this framework, the DSO can plan beyond the investments strictly required to ensure distribution grid security and explore additional investment options to reduce the netload range at the substation. These options require extra capital costs ($\Delta\Gamma$) and result in a narrower substation netload when compared to a conventional distribution planning. The NRCC is the organization of these *"netload range vs capital cost"* to be used in the transmission planning process.

As illustrated on the lower-right figure of Fig. 1, increasing the distribution planning cost from $\Delta\Gamma_1$ to $\Delta\Gamma_3$ allows the substation load profile to shift from the black curve to the blue curve. This shift significantly reduces the maximum netload range, narrowing it from $[\lambda^R(\Delta\Gamma_1), \lambda^D(\Delta\Gamma_1)]$ to $[\lambda^R(\Delta\Gamma_3), \lambda^D(\Delta\Gamma_3)]$, as highlighted by the upper-right NRCC curve. In our framework, the transmission planning model selects a specific load profile from the discrete options while balancing its own network upgrade investments. This provides transmission planners with an alternative to potentially defer or minimize costly transmission-side investments.

To compute the NRCC, three models are involved and computed in parallel or in sequence. In the following subsections, we present, in a compact form, a scenario-based distribution planning model and our proposed mathematical formulations for NRCC-related distribution and transmission planning models.

B. Scenario-Based Least-Cost Distribution Network Planning Under DER Growth Uncertainty

First, we present the scenario-based least-cost distribution network planning (LCDNP) model, which assumes the distribution network planners select their own investments which achieves the locally least costs, without taking into account the associated impacts on the connected transmission grid. In this formulation, different distribution netload scenarios are considered to incorporate multiple plausible future trajectories of behind-the-meter DER growth and load increase. This LCDNP model will serve as the prerequisite for our proposed TADNP model and the calculation of NRCCs, ensuring the secure and cost-effective operation under different DER growth conditions. The compact scenario-based LCDNP formulation is presented as below:

$$\Gamma^0 = \min_{\boldsymbol{u},\boldsymbol{v},\boldsymbol{w}_s} \; F^{\mathrm{DN}}(\boldsymbol{u},\boldsymbol{v},\{\boldsymbol{w}_s\}_{s\in\mathcal{S}}) \tag{1a}$$

$$\text{s.t.}: \quad (\boldsymbol{u},\boldsymbol{v}) \in \mathcal{X}^{\mathrm{pl}} \tag{1b}$$

$$(\boldsymbol{w}_s) \in \mathcal{X}_s^{\mathrm{op}}(\boldsymbol{u},\boldsymbol{v}), s \in \mathcal{S} \tag{1c}$$

$$u \in \{0,1\}, v \in \mathbb{R}_+, \tag{1d}$$

where the objective function to be minimized in (1a) comprises the total investment cost of the DSO, whose optimal value is assigned to Γ^0, which we refer to as *the least-cost feasible budget* hereafter. Vector $\boldsymbol{u}$ contains binary decision variables associated with investments for resource allocation and replacement, such as line reinforcement, voltage regulator (VR) placement, and feeder head upgrade, while vector $\boldsymbol{v}$ is composed of continuous decision variables representing capacity investment, such as storage sizing and allocation. Vector $\boldsymbol{w}_s$ comprises all operational decision variables related to scenario s. Set $\mathcal{X}^{\mathrm{pl}}$ in (1b) gathers all constraints related to planning investments, while set $\mathcal{X}_s^{\mathrm{op}}(\boldsymbol{u},\boldsymbol{v})$ in (1c) represents the feasible set for power system operation under the scenario s, given the investment $(\boldsymbol{u},\boldsymbol{v})$.

C. Transmission-Aware Distribution Network Planning Model

As previously discussed, the LCDNP model focuses solely on least-cost solutions to ensure distribution grid security under all potential future DER growth scenarios, neglecting its impact on the transmission system. However, well-designed incentive mechanisms can encourage DSOs to implement additional upgrades beyond those required for feasible network operation under load growth scenarios to support TSOs and, in turn, help society save millions of dollars in capital-intensive transmission investments. In our proposed framework, the costs of these additional upgrades are quantified as the *NRCC cost* $\Delta\Gamma_k$ in the DSO's investment budget. Since transmission planners typically base investment decisions on peak load conditions, strategically allocating $\Delta\Gamma_k$ to reduce peak loads at the distribution level offers a cost-effective approach to mitigating transmission investment needs. Within this context, we formulate our TADNP model as follows:

$$\min_{\boldsymbol{u},\boldsymbol{v},\boldsymbol{w_s},\boldsymbol{\lambda}} W[\lambda^D - \Lambda^D]^+ + (1-W)[\lambda^R - \Lambda^R]^+ \tag{2a}$$

$$\text{s.t.}: \quad (1b), (1c), (1d) \tag{2b}$$

$$-\lambda^R \leq p^{\text{up}}_{n,d,t,s} \leq \lambda^D, \forall n \in \mathcal{N}^{\text{sub}}, d \in \mathcal{D}, t \in \mathcal{T}, s \in \mathcal{S} \tag{2c}$$

$$(\lambda^D, \lambda^R) \in \mathbb{R}_+ \tag{2d}$$

$$F^{\text{DN}}(\boldsymbol{u}, \boldsymbol{v}, \{\boldsymbol{w}_s\}_{s\in\mathcal{S}}) \leq \Gamma^0 + \Delta\Gamma_k. \tag{2e}$$

The objective function to be minimized in (2a) is defined as the largest deviation of peak direct and reverse substation netloads across all possible realizations of DER adoption, λ^D and λ^R, relative to the expected direct and reverse netloads, Λ^D and Λ^R. $[\cdot]^+ = \max\{\cdot, 0\}$ reflects the positive-part function, while $W \in [0,1]$ is a user-defined weighting factor that prioritizes the penalties of direct or reverse peak netloads related to the expected RES growth scenario. The rationale behind this objective is that it reflects the maximum netloads that may materialize, thereby driving transmission-side reinforcement needs due to DER growth uncertainty.

More specifically, the parameters Λ^D and Λ^R represent the expected peak direct and reverse substation netloads in the absence of uncertainty in future DER adoption. Their values are obtained by solving the deterministic version of the LCDNP (1), where the scenario set $\mathcal{S}$ contains only one element, namely the expected DER adoption scenario s^0. Notably, since stochasticity is not considered, these values are unreliable for representing the future and serve only as reference points. On the other hand, the decision vector $\boldsymbol{\lambda} = [\lambda^D, \lambda^R]$ in the optimal solution of (2a) represents the maximum direct (D) and reverse (R) peak netloads among all considered DER growth scenarios. Their values are constrained by (2c), which accounts for substation netloads across all operational periods and DER growth scenarios. These values indicate transmission-side reinforcement needs if the resulting peaks cannot be accommodated by the existing infrastructure.

In addition to the investment and operational constraints (2b), which are also included in (1), our TADNP model imposes a limit on the total investment cost via constraint (2e) rather than optimizing it in the objective function. This limit is defined as the least-cost feasible budget Γ^0, obtained from the scenario-based LCDNP (1), plus an NRCC cost $\Delta\Gamma_k$. We define $\Delta\Gamma_k$ as the incentive provided by the TSO to the DSO to encourage a reduction in the netload range (we refer to this service as the *NRCC service* hereafter). In our framework, from the DSO's perspective, K possible NRCC service options can be obtained by adjusting the values of $\Delta\Gamma_k$ ($k = 1, \ldots, K$) and iteratively solving the TADNP optimization problem (2) for each $\Delta\Gamma_k$. The resulting solutions yield a series of peak netload ranges, $[\lambda^R(\Delta\Gamma_k), \lambda^D(\Delta\Gamma_k)]$ ($k = 1, \ldots, K$), each corresponding to a specific network upgrade plan. With this information, the NRCCs can be constructed as shown in the upper right corner of Fig. 1. The corresponding time-series load profiles, $p^{\text{up}}_{n,d,t,s}(\Delta\Gamma_k)$, at each substation node $n \in \mathcal{N}^{\text{sub}}$ under each possible DER growth scenario s, can then be integrated into our proposed NRCC-informed transmission planning model.

It is worth noting that while the TADNP model (2) is scenario-based, the NRCC framework is independent of how reliability is modeled. Planners can add $N-k$ or extreme-event scenarios into $\mathcal{S}$, or adopt a robust approach by defining a net-load uncertainty set and dropping the scenario index s from the operational variables, leaving all other equations unchanged. This flexibility lets each utility tailor the framework to its own risk tolerance and reliability standards.

We acknowledge that the proposed TADNP model, as formulated in (2), treats netload profiles as exogenous inputs, a common simplification in long-term planning models. In reality, end-user behavior, including load consumption, DER adoption, and demand response, may be influenced by electricity rates and price signals, which can themselves be affected by grid investment decisions. Modeling this endogenous relationship would require integrating tariff design and user choice models into the planning framework, significantly increasing its complexity. While this would unlock additional flexibility and potentially lead to more cost-effective NRCCs, the current simplification allows for a clear introduction of the core NRCC concept. A full treatment of this endogeneity is a promising direction for future research.

D. NRCC-Informed Transmission Planning Model

Given computed NRCCs and corresponding load profiles, we formulate the NRCC-informed transmission planning model as follows:

$$\min_{\boldsymbol{u}^\dagger,\boldsymbol{v}^\dagger,\boldsymbol{w}^\dagger_s,\boldsymbol{x}^{\text{NRCC},\dagger}} F^{\text{TN}}(\boldsymbol{u}^\dagger, \boldsymbol{v}^\dagger, \boldsymbol{w}^\dagger_s) + \sum_{i\in\mathcal{N}^{\text{TN}}}\sum_{k\in\mathcal{K}} \Delta\Gamma_{i,k} x^{\text{NRCC},\dagger}_{i,k} \tag{3a}$$

$$\text{s.t.}: \quad (\boldsymbol{u}^\dagger, \boldsymbol{v}^\dagger) \in \mathcal{X}^{\text{pl},\dagger} \tag{3b}$$

$$\boldsymbol{w}^\dagger_s \in \mathcal{X}^{\text{op},\dagger}_s(\boldsymbol{u}^\dagger, \boldsymbol{v}^\dagger), \forall s \in \mathcal{S} \tag{3c}$$

$$\sum_{k\in\mathcal{K}} x^{\text{NRCC},\dagger}_{i,k} \leq 1, \forall i \in \mathcal{N}^{\text{TN}} \tag{3d}$$

$$x^{\text{NRCC},\dagger}_{i,k} \in \{0,1\}, \forall i \in \mathcal{N}^{\text{TN}}, k \in \mathcal{K} \tag{3e}$$

$$D^{\text{load},\dagger}_{i,d,t,s} = D^{\text{load},0}_{i,d,t,s} + \sum_{k\in\mathcal{K}} \Big[p^{\text{sub}}_{i,d,t,s}(\Delta\Gamma_{i,k}) - D^{\text{load},0}_{i,d,t,s}\Big] x^{\text{NRCC},\dagger}_{i,k}, \quad \forall i \in \mathcal{N}^{\text{TN}}, d \in \mathcal{D}, t \in \mathcal{T}, s \in \mathcal{S} \tag{3f}$$

In the objective function (3a), the first term, $F^{\mathrm{TN}}(\boldsymbol{u}^{\dagger}, \boldsymbol{v}^{\dagger}, \boldsymbol{w}_s^{\dagger})$, represents the cost of regular infrastructure reinforcement $\boldsymbol{u}^{\dagger}$ and resource allocation $\boldsymbol{v}^{\dagger}$. Additionally, the second term incorporates the cost associated with NRCC services. When $x_{i,k}^{\mathrm{NRCC},\dagger} = 1$, it means the k-th option is purchased at transmission node q, with the associated node-specific NRCC cost $\Delta\Gamma_{i,k}$. Furthermore, in addition to the planning and operational constraints, i.e., (3b) and (3c), (3d) and (3e) ensure that only one specific NRCC service is selected from the DSO connected to each transmission node $n \in \mathcal{N}^{\mathrm{TN}}$. Lastly, constraint (3f) defines the resulting demand at node n after the NRCC service is selected from the connected DSO, where the original netload level $D_{i,d,t,s}^{\mathrm{load},0}$ is changed to $p_{i,d,t,s}^{\mathrm{sub}}(\Delta\Gamma_{i,k})$ by purchasing the k-th NRCC service. Note that the load profile $p_{i,d,t,s}^{\mathrm{sub}}(\Delta\Gamma_{i,k})$ supplied with each NRCC option k actually gives the TSO concrete "stress case" scenarios [28], as it is obtained from a dispatch simulation in the TADNP (2) that respects all distribution constraints across $s \in \mathcal{S}$. In addition, limiting the NRCC menu to $|\mathcal{K}|$ discrete options keeps the transmission optimization manageable, as only a few options need to be evaluated, reducing the computational burden. It is worth mentioning nonetheless that the NRCC framework itself does not limit the total number of options and their granularity. A DSO could add or remove options without changing the way NRCCs are built or used in the transmission planning. In addition, it is common practice that utilities bundle upgrades into a handful of discrete standard packages, as doing so simplifies managerial and engineering effort [29].

Compared to traditional uncoordinated planning processes, our proposed framework requires only the exchange of substation-level netload profile and NRCC between the TSO and DSOs, which is the information captured in constraints (3d)–(3f). Similar to the TADNP (2), the planning and operational layers (3b)–(3c) remain independent of the NRCC constraints (3d)–(3f), so model (3) can be refined to any desired detail. In Appendix A, we provide our full formulation used here, and higher-fidelity elements such as AC power-flow constraints or alternative reliability criteria can be incorporated when necessary.

E. Steps for Implementing the NRCC in the T&D Planning

To derive the NRCC, the DSO runs the TADNP model, relying on long-term load growth and DER forecasts beyond the distribution planning cycle (these type of forecasts are already used in other distribution utility proceedings [30]). The NRCC costs can then be multiplied by a DSO "profit margin" (or "compensation" in regulated setups) and offered as product options for the TSO. The TSO then selects the point of the NRCC that is cost-effective for the transmission planning, using model (3). Within this framework, the DSO has an incentive to reduce the "profit margin" of the NRCC products to increase their chance to be included in the TSO planning. When the TSO purchases a service option of the NRCC, the DSO knows what corresponding distribution investments are needed to enable it.

After the transaction, there are two ways that a regulator can verify that the NRCC service was provided: i) ex-ante, the regulator can check whether the DSO made those investments; ii) ex-post, the TSO can check whether the netload at the substation remains within the NRCC values. These verification steps are crucial due to the inherent information asymmetry between DSOs and TSOs, as DSOs possess detailed knowledge of their network. To mitigate the risk of DSOs' overestimating costs or underestimating their capabilities, safeguards are necessary. These could include regular NRCC recalculations (e.g., every 2-3 years) to reflect actual DER growth, detailed engineering justifications for each option, independent audits, and penalties for non-compliance. However, a full design of these regulatory measures is beyond the scope of the present paper and will be explored in future work.

III. Mathematical Formulation and Solution Procedure of the TADNP Model

Building on the compact models presented in the previous section, this section provides a detailed mathematical formulation of the TADNP model (2), followed by an overview of our proposed T&D planning coordination methodology.

A. Mathematical Formulation of the TADNP Model

As the objective function (2a) and auxiliary constraints for maximum netloads (2c) are already presented in the last section, we are going to provide the details of the operation and planning constraints (2b) and the budget constraint (2e).

1) Budget Constraint: Below we express the detailed version of constraint (2e):

$$\begin{aligned}
&F^{\mathrm{DN}}(\boldsymbol{u}, \boldsymbol{v}, \{\boldsymbol{w}_s\}_{s\in\mathcal{S}}) \\
&= \Bigg\{ \sum_{(m,n)\in\mathcal{L}^{\mathrm{c}}} \sum_{r\in\Omega^{\mathrm{P}}} C_{mn,r}^{\mathrm{L}} x_{mn,r}^{\mathrm{L}} + \sum_{(m,n)\in\mathcal{L}^{\mathrm{VR}}} C_{mn}^{\mathrm{VR}} x_{mn}^{\mathrm{VR}} \\
&+ \sum_{n\in\mathcal{N}^{\mathrm{B}}} C_n^{\mathrm{st}} x_n^{\mathrm{st}} + \sum_{(m,n)\in\mathcal{L}^{\mathrm{FH}}} C_{mn}^{\mathrm{FH}} x_{mn}^{\mathrm{FH}} \\
&+ \sum_{n\in\mathcal{N}} \sum_{d\in\mathcal{D}} \sum_{t\in\mathcal{T}} \sum_{s\in\mathcal{S}} w_d \cdot \mathrm{prob}_s \cdot C^{I} (p_{n,d,t,s}^{I,+} \\
&+ p_{n,d,t,s}^{I,-} + q_{n,d,t,s}^{I,+} + q_{n,d,t,s}^{I,-}) \Bigg\} \le \Gamma^0 + \Delta\Gamma_k
\end{aligned} \tag{4}$$

The first four terms in (4) comprise costs related to line reconductoring, voltage regulator installation, storage placement, and feeder head transformer reinforcement. Since the analysis is performed at the feeder level, we apportion transformer upgrades relative to the feeder. The last term represents the penalty cost of load shedding, which aims to maintain operational feasibility under different DER growth scenarios.

2) Nodal Balance and Reference Voltage: Investment and operation constraints are expressed as follows.

$$\begin{aligned}
&P_{n,d,t,s}^{\mathrm{load}} + \sum_{m|(n,m)\in\mathcal{L}} p_{nm,,d,t,s}^{\mathrm{L}} - \sum_{m|(m,n)\in\mathcal{L}} p_{mn,d,t,s}^{\mathrm{L}} \\
&= \sum_{n\in\mathcal{N}^{\mathrm{sub}}} p_{n,d,t,s}^{\mathrm{sub}} + p_{n,d,t,s}^{\mathrm{st,d}} - p_{n,d,t,s}^{\mathrm{st,c}} + p_{n,d,t,s}^{\mathrm{I},+} \\
&\qquad - p_{n,d,t,s}^{\mathrm{I},-}, \forall n \in \mathcal{N}^{\mathrm{DN}}, d \in \mathcal{D}, t \in \mathcal{T}, s \in \mathcal{S}
\end{aligned} \tag{5}$$

$$Q^{\text{load}}_{n,d,t,s} + \sum_{m|(n,m)\in\mathcal{L}} q^{\text{L}}_{nm,d,t,s} - \sum_{m|(m,n)\in\mathcal{L}} q^{\text{L}}_{mn,d,t,s} = \sum_{n\in\mathcal{N}^{\text{sub}}} q^{\text{sub}}_{n,d,t,s} + q^{\text{st}}_{n,d,t,s} + q^{\text{I},+}_{n,d,t,s} - q^{\text{I},-}_{n,d,t,s}, \quad \forall n\in\mathcal{N}^{\text{DN}}, d\in\mathcal{D}, t\in\mathcal{T}, s\in\mathcal{S} \tag{6}$$

$$p^{I,+}_{n,d,t,s}, p^{I,-}_{n,d,t,s}, q^{I,+}_{n,d,t,s}, q^{I,-}_{n,d,t,s} \geq 0, \quad \forall n\in\mathcal{N}^{\text{DN}}, d\in\mathcal{D}, t\in\mathcal{T}, s\in\mathcal{S} \tag{7}$$

$$u^{\text{sqr}}_{n,d,t,s} = (u^{\text{ref}})^2, \forall n \in \mathcal{L}^{\text{FH}}, \quad \forall n\in\mathcal{N}^{\text{DN}}, d\in\mathcal{D}, t\in\mathcal{T}, s\in\mathcal{S} \tag{8}$$

$$\underline{U}^{\text{sqr}}_n \leq u^{\text{sqr}}_{n,d,t,s} \leq \overline{U}^{\text{sqr}}_n, \forall n\in\mathcal{N}^{\text{DN}}, d\in\mathcal{D}, t\in\mathcal{T}, s\in\mathcal{S} \tag{9}$$

where constraints (5) enforce active nodal balance for distribution nodes considering the load of each node, power flows in and out, potential local injection, storage devices, as well as slack variables that are penalized in the objective function. Constraints (6) play an analogous role for reactive balance. Constraint (7) enfore the non-negativity of slack variables. Voltage reference for each substation and voltage limits for all buses are imposed in (8) and (9), respectively.

3) Fixed and Candidate Line Segments:

$$\overline{S}^{\text{L}}_{mn} = \sum_{r\in\Omega^{\text{P}}} x^{\text{L}}_{mn,r}\text{cap}_{mn,r}, \forall (m,n)\in\mathcal{L}^{\text{c}} \tag{10}$$

$$\overline{S}^{\text{L}}_{mn} = \overline{S}^{\text{L,fixed}}_{mn}, \forall (m,n)\in\mathcal{L}\setminus\mathcal{L}^{\text{c}} \tag{11}$$

$$\sum_{r\in\Omega^{\text{P}}} x^{\text{L}}_{mn,r} = 1, \forall (m,n)\in\mathcal{L}^{\text{c}} \tag{12}$$

$$-\overline{S}^{\text{L}}_{mn} \leq p^{\text{L}}_{mn,d,t,s} \leq \overline{S}^{\text{L}}_{mn}, \forall (m,n)\in\mathcal{L}, d\in\mathcal{D}, t\in\mathcal{T}, s\in\mathcal{S} \tag{13}$$

$$-\overline{S}^{\text{L}}_{mn} \leq q^{\text{L}}_{mn,d,t,s} \leq \overline{S}^{\text{L}}_{mn}, \forall (m,n)\in\mathcal{L}, d\in\mathcal{D}, t\in\mathcal{T}, s\in\mathcal{S} \tag{14}$$

$$q^{\text{L}}_{mn,d,t,s} \leq \overline{f}^q(p^{\text{L}}_{mn,d,t,s}, \overline{S}^{\text{L}}_{mn}, e), \forall (m,n)\in\mathcal{L}, d\in\mathcal{D}, t\in T, s\in\mathcal{S}, e\in\{1,\ldots,4\} \tag{15}$$

$$-q^{\text{L}}_{mn,d,t,s} \leq \overline{f}^q(p^{\text{L}}_{mn,d,t,s}, \overline{S}^{\text{L}}_{mn}, e), \forall (m,n)\in\mathcal{L}, d\in\mathcal{D}, t\in T, s\in\mathcal{S}, e\in\{1,\ldots,4\} \tag{16}$$

$$-(1-x^{\text{L}}_{mn,r})M \leq u^{\text{sqr}}_{n,d,t,s} - \Big[u^{\text{sqr}}_{m,d,t,s} - 2(R_{mn,r}p^{\text{L}}_{mn,d,t,s} + X_{mn,r}q^{\text{L}}_{mn,d,t,s})\Big] \leq (1 - x^{\text{L}}_{mn,r})M, \forall (m,n)\in\mathcal{L}^{\text{c}}, d\in\mathcal{D}, t\in\mathcal{T}, s\in\mathcal{S}, r\in\Omega^{\text{P}} \tag{17}$$

$$u^{\text{sqr}}_{n,d,t,s} - \Big[u^{\text{sqr}}_{m,d,t,s} - 2(R_{mn}p^{\text{L}}_{mn,d,t,s} - + X_{mn}q^{\text{L}}_{mn,d,t,s})\Big] = 0, \forall (m,n)\in\mathcal{L}\setminus\mathcal{L}^{\text{c}}, d\in\mathcal{D}, t\in\mathcal{T}, s\in\mathcal{S} \tag{18}$$

where $\overline{f}^q(p^{\text{L}}_{mn,d,t,s}, \overline{S}^{\text{L}}_{mn}, e) = cotan((\frac{1}{2}-e)\frac{\pi}{4})\cdot(p^{\text{L}}_{mn,d,t,s} - \cos(\frac{\pi}{4}e)\cdot\overline{S}^{\text{L}}_{mn}) + \sin(\frac{\pi}{4}e)\cdot\overline{S}^{\text{L}}_{mn}$. Expressions (10) and (12) model the potential selection of an upgrade option for each line segment $(m,n)\in\mathcal{L}^{\text{c}}$ while (11) enforces a fixed capacity for lines that are not candidate for reinforcement. It is worth mentioning that one of the options is to keep line segment l unaltered, whose respective cost C^r_{mn} is null. Depending on the values of decision variables $x^{\text{L}}_{mn,r}$, the power flow limits are considered in (13)–(15) and the respective resistances and reactances are taken into account for voltage drop in (17) and (18).

4) Constraints for Tap Changing:

$$\frac{u^{\text{sqr,mid}}_{n,d,t,s}}{(\varphi^{\max}_{mn})^2}, \leq u^{\text{sqr}}_{n,d,t,s} \leq \frac{u^{\text{sqr,mid}}_{n,d,t,s}}{(\varphi^{\min}_{mn})^2}, \quad \forall (m,n)\in\mathcal{L}^{\text{VR}}\cup\mathcal{L}^{\text{FH}}, d\in\mathcal{D}, t\in\mathcal{T}, s\in\mathcal{S} \tag{19}$$

$$-Mx^{\text{VR}}_{mn} \leq u^{\text{sqr,mid}}_{n,d,t,s} - u^{\text{sqr}}_{n,d,t,s} \leq Mx^{\text{VR}}_{mn}, \quad \forall (m,n)\in\mathcal{L}^{\text{VR}}, d\in\mathcal{D}, t\in\mathcal{T}, s\in\mathcal{S} \tag{20}$$

$$x^{\text{VR}}_{mn} \in \{0,1\}, \forall (m,n)\in\mathcal{L}^{\text{VR}} \tag{21}$$

We account for the possibility of tap changing in VRs and on-load tap changer (OLTC) transformers located at the feeder head. Here, $u^{\text{sqr,mid}}_{n,d,t,s}$ represents the squared voltage at an internal "mid-tap" virtual node introduced inside each VR or transformer. This virtual node captures the effect of the tap ratio while leaving the external node pair (m,n) unchanged in the network model. In this context, expression (19) defines the constraints on tap changing. Additionally, expressions (20) and (21) model the logic governing the activation of tap adjustments for candidate VRs selected for installation.

5) Constraints for Feeder Head and Voltage Regulators:

$$\overline{S}^{\text{L}}_{mn} = \overline{S}^{\text{FH,fixed}}_{mn} + x^{\text{FH}}_{mn}\Delta S^{\text{FH}}_{mn}, \forall (m,n)\in\mathcal{L}^{\text{FH}} \tag{22}$$

$$\overline{S}^{\text{L}}_{mn} = \overline{S}^{\text{VR,fixed}}_{mn}, \forall (m,n)\in\mathcal{L}^{\text{VR}} \tag{23}$$

$$-\overline{S}^{\text{L}}_{mn} \leq p^{\text{L}}_{mn,d,t,s} \leq \overline{S}^{\text{L}}_{mn}, \forall (m,n)\in\mathcal{L}^{\text{VR}}\cup\mathcal{L}^{\text{FH}}, d\in\mathcal{D}, t\in\mathcal{T}, s\in\mathcal{S} \tag{24}$$

$$-\overline{S}^{\text{L}}_{mn} \leq q^{\text{L}}_{mn,d,t,s} \leq \overline{S}^{\text{L}}_{mn}, \forall (m,n)\in\mathcal{L}^{\text{VR}}\cup\mathcal{L}^{\text{FH}}, d\in\mathcal{D}, t\in\mathcal{T}, s\in\mathcal{S} \tag{25}$$

$$q^{\text{L}}_{mn,d,t,s} \leq \overline{f}^q(p^{\text{L}}_{mn,d,t,s}, \overline{S}^{\text{L}}_{mn}, e), \quad \forall (m,n)\in\mathcal{L}^{\text{VR}}\cup\mathcal{L}^{\text{FH}}, d\in\mathcal{D}, t\in T, s\in\mathcal{S}, e\in\{1,\ldots,4\} \tag{26}$$

$$-q^{\text{L}}_{mn,d,t,s} \leq \overline{f}^q(p^{\text{L}}_{mn,d,t,s}, \overline{S}^{\text{L}}_{mn}, e), \quad \forall (m,n)\in\mathcal{L}^{\text{VR}}\cup\mathcal{L}^{\text{FH}}, d\in\mathcal{D}, t\in T, s\in\mathcal{S}, e\in\{1,\ldots,4\} \tag{27}$$

$$-x^{\text{FH}}_{mn}M \leq u^{\text{sqr,mid}}_{n,d,t,s} - \Big[u^{\text{sqr}}_{m,d,t,s} - 2(R^{FH}_{mn}p^{\text{L}}_{mn,d,t,s} + X^{FH}_{mn}q^{\text{L}}_{mn,d,t,s})\Big] \leq x^{\text{FH}}_{mn}M,$$

$$\forall(m,n) \in \mathcal{L}^{\mathrm{FH}}, d \in \mathcal{D}, t \in \mathcal{T}, s \in \mathcal{S} \quad (28)$$

$$-(1-x^{\mathrm{FH}}_{mn})M \leq u^{\mathrm{sqr,mid}}_{n,d,t,s} - \Big[u^{\mathrm{sqr}}_{m,d,t,s} - 2(R^{FH\dagger}_{mn} p^{\mathrm{L}}_{mn,d,t,s} + X^{FH\dagger}_{mn,r} q^{\mathrm{L}}_{mn,d,t,s})\Big] \leq (1 - x^{\mathrm{FH}}_{mn,r})M, \forall(m,n) \in \mathcal{L}^{\mathrm{FH}}, d \in \mathcal{D}, t \in \mathcal{T}, s \in \mathcal{S} \quad (29)$$

$$u^{\mathrm{sqr,mid}}_{n,d,t,s} - \Big[u^{\mathrm{sqr}}_{m,d,t,s} - 2(R_{mn} p^{\mathrm{L}}_{mn,d,t,s} + X_{mn} q^{\mathrm{L}}_{mn,d,t,s})\Big] = 0, \forall(m,n) \in \mathcal{L}^{\mathrm{VR}}, d \in \mathcal{D}, t \in \mathcal{T}, s \in \mathcal{S} \quad (30)$$

$$x^{\mathrm{FH}}_{mn} \in \{0,1\}, \forall(m,n) \in \mathcal{L}^{\mathrm{FH}} \quad (31)$$

Expressions (22) and (23) determine the capacities of feeder head transformers and VRs, respectively. Based on these capacities, power flow limits are enforced in (24)–(27). Moreover, constraints (28)–(30) represent voltage drop while (31) expresses the binary nature of x^{FH}_{mn}.

6) Constraints for Storage Operation:

$$0 \leq p^{\mathrm{st,c}}_{n,d,t,s} \leq \overline{P}^{\mathrm{st,c}}_{n} x^{\mathrm{st}}_{n}, \forall n \in \mathcal{N}^{\mathrm{B}}, d \in \mathcal{D}, t \in T, s \in \mathcal{S} \quad (32)$$

$$0 \leq p^{\mathrm{st,d}}_{n,d,t,s} \leq \overline{P}^{\mathrm{st,d}}_{n} x^{\mathrm{st}}_{n}, \forall n \in \mathcal{N}^{\mathrm{B}}, d \in \mathcal{D}, t \in T, s \in \mathcal{S} \quad (33)$$

$$p^{\mathrm{st,c}}_{n,d,t,s} = 0,\ p^{\mathrm{st,d}}_{n,d,t,s} = 0, \forall n \in \mathcal{N}^{\mathrm{DN}} \setminus \mathcal{N}^{\mathrm{B}}, d \in \mathcal{D}, t \in T, s \in \mathcal{S} \quad (34)$$

$$-\psi_n \overline{P}^{\mathrm{st,c}} x^{\mathrm{st}}_{n} \leq q^{\mathrm{st}}_{n,d,t,s} \leq \psi_n \overline{P}^{\mathrm{st,c}} x^{\mathrm{st}}_{n}, \forall n \in \mathcal{N}^{\mathrm{B}}, d \in \mathcal{D}, t \in T, s \in \mathcal{S} \quad (35)$$

$$e^{\mathrm{st}}_{n,d,t,s} = e^{\mathrm{st,ini}}_{n,d,s} + \eta^{\mathrm{c}}_{n} p^{\mathrm{st,c}}_{n,d,t,s}\Delta t - (1/\eta^{\mathrm{d}}_{n}) p^{\mathrm{st,d}}_{n,d,t,s}\Delta t, \forall n \in \mathcal{N}^{\mathrm{B}}, d \in \mathcal{D}, t = t^{\mathrm{ini}}_{d}, s \in \mathcal{S} \quad (36)$$

$$e^{\mathrm{st}}_{n,d,t,s} = e^{\mathrm{st}}_{n,d,t-1,s} + \eta^{\mathrm{c}}_{n} p^{\mathrm{st,c}}_{n,d,t,s}\Delta t - (1/\eta^{\mathrm{d}}_{n}) p^{\mathrm{st,d}}_{n,d,t,s}\Delta t, \forall n \in \mathcal{N}^{\mathrm{B}}, d \in \mathcal{D}, t \in \mathcal{T} | t \neq t^{\mathrm{ini}}_{d}, s \in \mathcal{S} \quad (37)$$

$$e^{\mathrm{st}}_{n,d,t,s} = e^{\mathrm{st,ini}}_{n,d,s}, \forall n \in \mathcal{N}^{\mathrm{B}}, d \in \mathcal{D}, t = t^{\mathrm{last}}_{d}, s \in \mathcal{S} \quad (38)$$

$$0 \leq e^{\mathrm{st}}_{n,d,t,s} \leq T^{\mathrm{st}}_{n} \overline{P}^{\mathrm{st,c}}_{n} x^{\mathrm{st}}_{n}, \forall n \in \mathcal{N}^{\mathrm{B}}, d \in \mathcal{D}, t \in \mathcal{T}, s \in \mathcal{S} \quad (39)$$

Constraints (32)–(35) impose active and reactive power limits for storage devices, while also determining the installation and sizing of candidate storage units. Constraints (36)–(38) model the evolution of the state of charge (SoC) over time periods. Finally, constraints (39) define the upper and lower bounds on the SoC for the candidate storage units.

Therefore, the complete TADNP model is formulated with the objective function (2a) and constraints (4)–(39), (2c)–(2d).

B. Implementing Procedure for the Proposed Coordinated T&D Planning

Fig. 2 outlines the step-by-step implementation process of the proposed NRCC-integrated T&D coordination framework. The process is structured into four main steps:

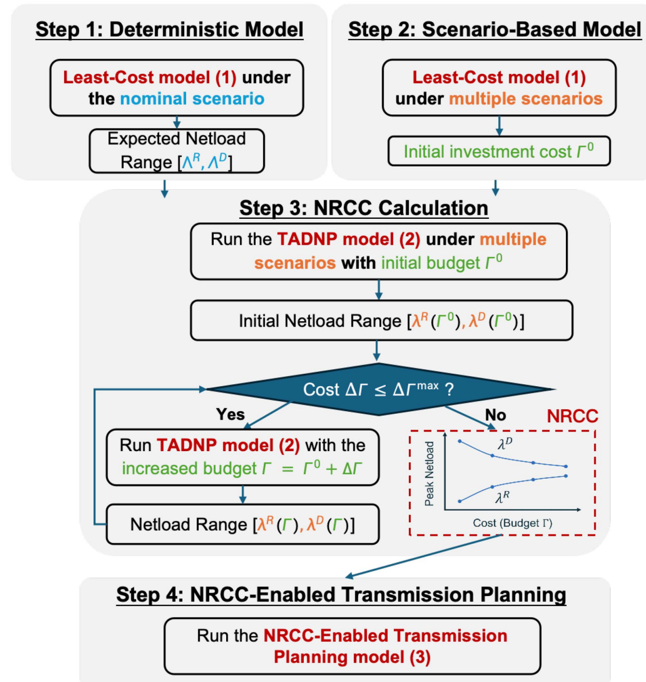

Fig. 2. Iteration-based solution procedure for NRCC computation.

Step 1. Deterministic LCDNP: Given the candidate investment set, we solve problem (1) using only the nominal scenario s^0, referred to hereafter as the *deterministic LCDNP model*. This step yields the expected netload range, $[\Lambda^R, \Lambda^D]$, which provides insights into expected peak direct and reverse netload demands at the substation. These values serve as inputs for the objective function (2a) of the TADNP model.

Step 2. Scenario-Based LCDNP: In parallel with Step 1 and using the same candidate set, the scenario-based LCDNP is solved while considering multiple scenarios to account for DER growth uncertainty. This step also determines the least-cost feasible budget Γ^0 required to upgrade the distribution system so as to ensure feasibility across the DER growth scenarios under consideration. In our framework, Γ^0 serves as the initial budget used in the budget constraints (2e) for the NRCC computation.

Step 3. NRCC Calculation Based on TADNP: Starting from the netload range $[\Lambda^R, \Lambda^D]$ and the least-cost feasible budget Γ^0 from the step 1 and 2, our procedure evaluates the impact of increasing the investment budget by $\Delta\Gamma$ on the netload range at substations. More specifically, starting with the initial investment Γ^0, the budget is iteratively increased by $\Delta\Gamma$ until the cost increment $\Delta\Gamma$ exceeds a predefined maximum allowable value $\Delta\Gamma^{\max}$. For each budget level $\Gamma = \Gamma^0 + \Delta\Gamma$, the netload range $[\lambda^R(\Gamma), \lambda^D(\Gamma)]$ is computed, enabling the construction of the NRCC. The NRCC quantifies the trade-offs between investment budgets and the ability of DSOs to manage netload deviations from the expected value.

Step 4. NRCC-Informed Transmission Planning: In the final step, the NRCC-informed transmission planning model (3) integrates the NRCC results from different DSOs connected to its nodes. In this way, transmission planners can explore the

TABLE I
PARAMETERS OF DISTRIBUTION NETWORKS FOR NRCC COMPUTATION

Substation Name	Number of Feeders/Buses/ Lines	Min/Max Netload (MW)	Min/Ave/Max Installed RPV (MW)
p3uhs9_1247	2/283/235	-3.53/10.10	2.19/6.33/7.85
p5uhs31_1247	5/901/734	0.48/13.59	2.28/3.58/6.46
p7uhs8_1247	4/585/518	-2.34/10.29	8.76/8.87/9.54
p14uhs9_1247	6/966/778	-1.46/16.02	3.55/7.26/12.08
p16uhs23_1247	5/2070/1683	-0.16/7.19	1.92/3.14/5.63
p21uhs5_1247	4/540/493	-0.43/23.19	13.18/13.28/13.29

feasibility of deferring costly transmission-side reinforcements by procuring NRCC services from DSOs, while maintaining overall system operational feasibility and security. This step underscores the non-intrusive coordination between T&D systems under long-term DER growth uncertainty.

IV. Numerical Results

In this section, we present case studies using the realistic networks located in San Francisco Bay Area. In Section IV.A, we introduce the general settings used for the study. As our proposed methodology starts from generating the NRCCs for substation-level distribution networks, in Section IV.B, we present TADNP results, including the NRCCs of two representative distribution networks and their corresponding network upgrades under different investment budgets. With the NRCC services calculated and passed from the distribution networks, the transmission system planning results are presented in Section IV.C to demonstrate the efficiency of NRCC adoption in deferring costly transmission-side investments.

A. System Setup

The distribution systems and transmission system used for numerical tests are based on the San Francisco distribution networks provided in the SmartDS dataset [31], and California Test System [32], respectively. Transmission and distribution systems are interconnected with substations, whose netload profiles and NRCCs are transmitted from the corresponding DSOs to the TSO. To simulate NRCCs of different TN nodes, we utilized 6 distribution networks located in San Francisco from SmartDS dataset, whose parameters are presented in Table I. Results from two representative distribution networks located in the San Mateo County in the San Francisco Bay Area, i.e., p7uhs8_1247 and p21uhs5_1247 (denoted as Distribution Network 1 and 2), will be presented and analyzed in Section IV.B, whose layouts are shown in Fig. 3. The two systems have 10/2/6 and 15/4/1 candidate lines/BESSs/VRs, respectively. Parameters and costs associated with candidate line reinforcements, BESSs, and VRs on the distribution network side are extracted from [33], [34]. The transmission network covering the San Francisco Bay Area consists of 163 nodes and 196 lines. The parameters and locations of the installed generators and BESSs on the transmission side are provided in [35]. Network and candidate parameters for both distribution networks and transmission networks can be accessed in [36]. To match the loading level of the transmission system, we randomly assign the substation-level netload profiles

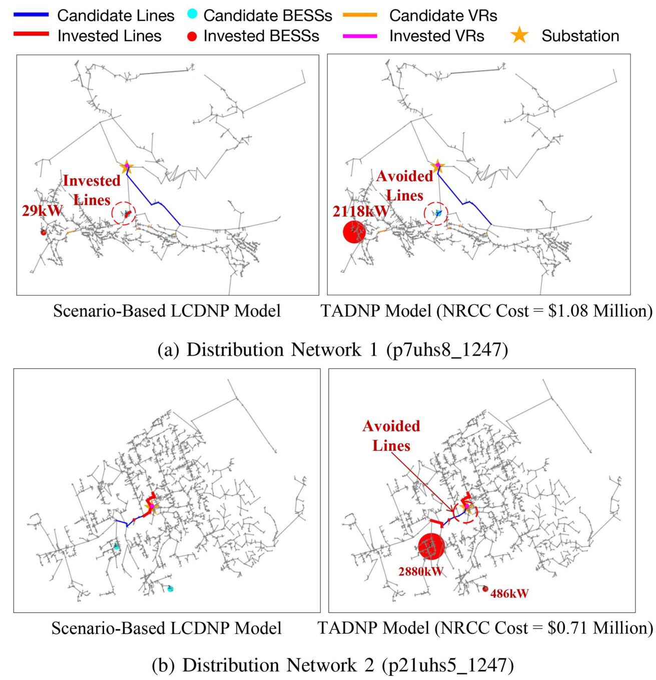

Fig. 3. Layout of distribution networks with candidates and investments.

computed from the 6 distribution networks to different transmission nodes and scale the NRCC and netload levels to match the original transmission nodes' load demands. Here we consider a 20-year planning horizon in the simulations, while the expected load demand is scaled to the projected level for 20 years, as forecasted by Cambium [37]. Another assumption in the case study is that every substation connected to the transmission nodes can offer NRCC services with three discrete options, each of which corresponds to a specific NRCC cost, peak substation-level netload range, and a related time-series netload profile. We chose a uniform, three-option menu so we could clearly show the effect of NRCCs on transmission planning. Nonetheless, the framework is flexible to add or remove options, as a DSO may offer fewer or more discrete options without changing the way NRCCs are generated or used.

In this case study, we assume that long-term netload uncertainty arises from general load growth and the adoption of behind-the-meter rooftop solar. This assumption allows us to illustrate how NRCCs handle uncertainty in both netload increases and decreases, and to show that the method is applicable regardless of the type of DER considered. Accounting for the load uncertainty, three load growth scenarios with different growth rates per year are considered: Low (1.5%), Medium (2.5%) and High (3.5%). Regarding DER growth scenario generation, we adopt innovation diffusion theory [38] to characterize how the RPV is adopted over time in the form of aggregate dynamics. For their geographical distributions, we utilize an agent-based simulation framework [39]. Through this method, we generate 100 future RPV growth scenarios and combine them with 3 future load growth scenarios to yield 300 netload scenarios in total. Then, by utilizing the hierarchical clustering

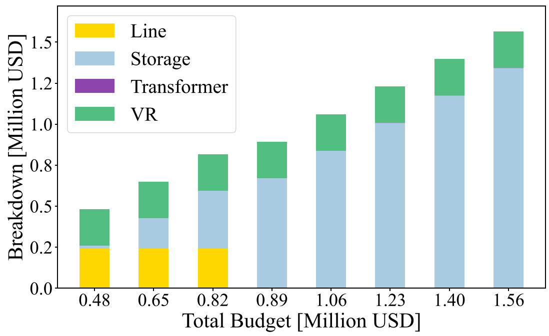

(a) Budget breakdown for Distribution Network 1

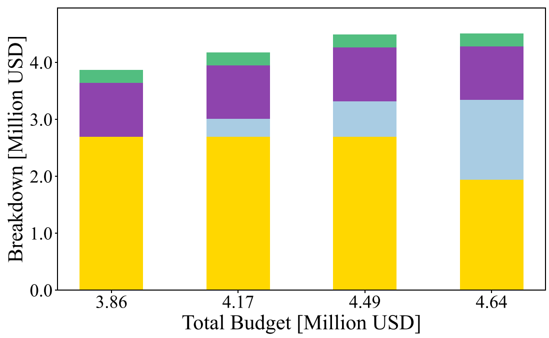

(b) Budget breakdown for Distribution Network 2

Fig. 4. Budget breakdowns.

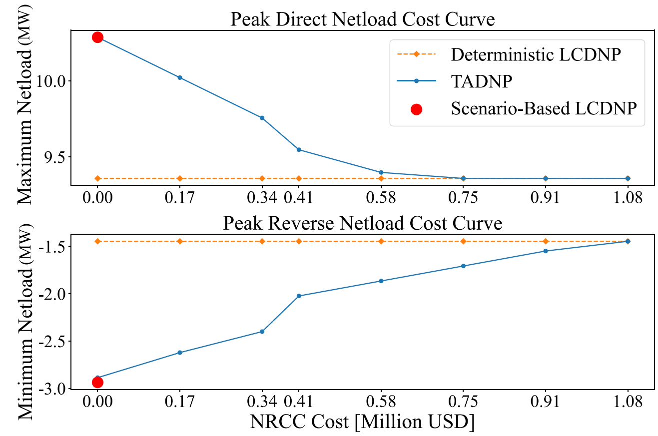

(a) NRCC for Distribution Network 1

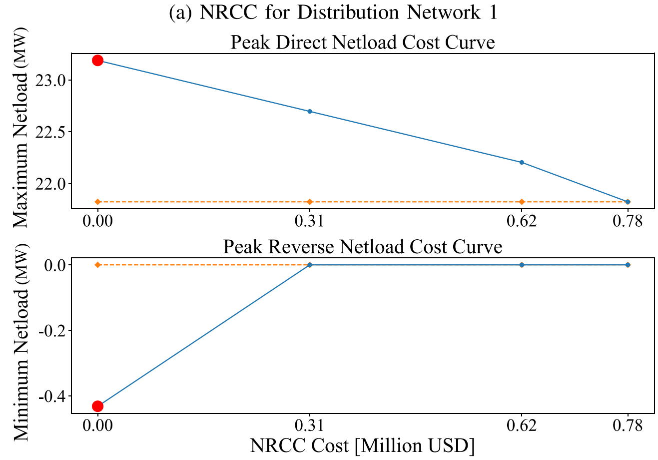

(b) NRCC for Distribution Network 2

Fig. 5. Netload range cost curves at substations.

method [40], those scenarios are reduced to 3 scenarios based on the information of their aggregate capacity and locations. Note that our framework is compatible with other scenario generation techniques for the DER growth. Furthermore, three representative days that are associated with the highest, average and lowest peak netload values are picked up for the case studies, which is aligned with usual approaches adopted in the technical literature [41].

B. Results of the TADNP and NRCCs on the Distribution Side

1) Budget Breakdowns: We first examine how budget increases influence investments within distribution networks. Fig. 4 illustrates the budget breakdowns for various investment types across different budget levels for Distribution Network 1 and 2. In Distribution Network 1, as the investment budget increases, more BESSs are installed. Initial investments in line upgrades are replaced by BESS installations once the budget reaches \$0.89 million. As shown in Fig. 3(a), when the budget increases to \$1.56 million, reinforcement on two lines is avoided, and the installed BESS capacity grows significantly from 29 kW to 2118 kW. These findings suggest that increased BESS capacity can effectively manage line power flow, eliminating the need for local infrastructure upgrades. A similar trend is observed in Distribution Network 2, where line reinforcements are partially replaced by increased BESS installations as the budget grows. At a budget of \$4.57 million, two BESSs with capacities of 2880 kW and 486 kW are installed, avoiding the one line reconductoring which would have cost \$0.75 million.

2) NRCCs: We then present the compiled NRCCs, and analyze how peak netload ranges at the substation change with varying distribution investment plans shown above. Instead of using the investment budget, we adopt the NRCC cost as the horizontal axis to explicitly denote the additional funding the DSO could potentially receive from the TSO. NRCCs for the two distribution networks are shown in Fig. 5. The blue lines in the upper and lower plots show the peak direct and reverse netloads obtained from the TADNP model, while the dashed orange lines and red dots depict the corresponding values from the deterministic LCDNP and scenario-based LCDNP models under nominal and multiple scenarios, respectively. These serve as references to demonstrate how the peak netload ranges under the TADNP model decrease as the TSO allocates more funding to the DSO.

Notably, when DSOs adopt the least-cost investments without considering the transmission side i.e., NRCC cost is 0, significant discrepancies exist between the peak substation-level netloads obtained from the deterministic and scenario-based LCDNP models, as the gaps between red dots and dashed lines indicate. This suggests the potential necessity for TSO investments to address uncertainties related to future DER growth. As the NRCC cost increases, the peak netloads progressively

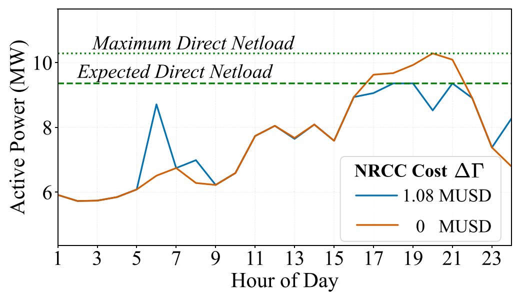

(a) Maximum netload scenario on the peak day at Substation 1

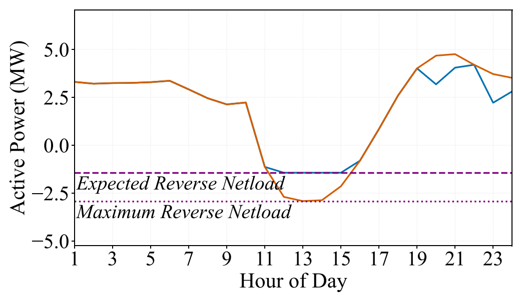

(b) Minimum netload scenario on the light-load day at Substation 1

Fig. 6. Substation-level load profiles in Distribution Network 1 under selected scenarios for representative days, with and without the NRCC-related investments.

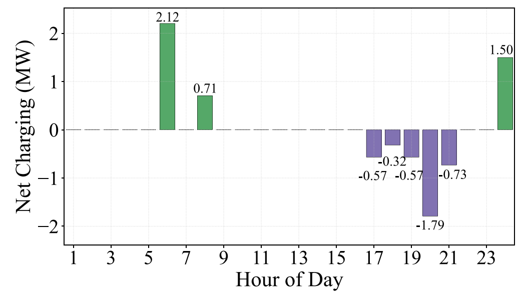

(a) Maximum netload scenario on the peak day

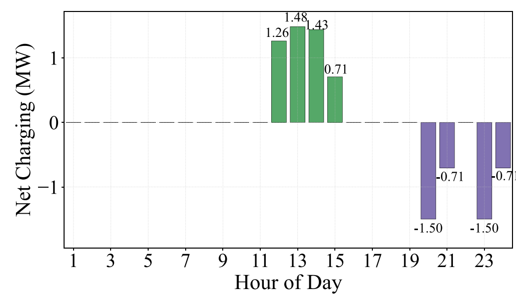

(b) Minimum netload scenario on the light-load day

Fig. 7. Net charging profiles of aggregated storage units in Distribution Network 1 under selected scenarios for representative days, with the NRCC-related investment ($\Delta\Gamma = 1.08$ Million USD).

converge to the expected values. With reference to the investment results and budget breakdowns in Figs. 3 and 4, we observe that this convergence is primarily driven by the deployment of new BESSs within distribution networks. BESSs effectively manage line power flows, minimizing local infrastructure upgrades while also reducing peak netload at the substation. These findings underscore the potential for offsetting the high costs of BESS installations through NRCC services, incentivized by additional funding from the TSO, therefore contributing to greater cost-effectiveness and enhanced social welfare.

3) Daily Load Profiles and BESS Net-Charging Patterns: To elucidate how NRCCs narrow the netload envelope, Fig. 6 plots the hourly netload at Substation 1 in the Distribution Network 1 on two representative days, with NRCC-related investment cost $\Delta\Gamma = 1.08$ Million USD and without NRCC-related investments. Fig. 7 presents the corresponding aggregate BESS net-charging schedules produced by the optimal dispatch after an NRCC option is selected.

On the peak day shown in Fig. 6(a), with NRCC, the evening crest is shaved from 10.3 MW to 9.3 MW, accounting for a 9.7% reduction, and the 17:00–21:00 interval is flattened so that every point stays beneath the expected direct netload benchmark. Fig. 7(a) reveals how BESSs achieve this effect: they charge during the early-morning surplus, then discharge through the peak, and take a brief charge at 23:00 to restore their SoCs. Similarly, on the light-load day with significant reverse flow, the maximum export shrinks from -2.9 to -1.4 MW with the NRCC service, while exports between 11:00 and 16:00 are held below the expected reverse netload baseline.

TABLE II
NUMERICAL RESULTS OF TN PLANNING MODEL WITH AND WITHOUT NRCCS

	w/o NRCC	with NRCC
Investment Cost (Million \$)	1129.45	943.03
No. of Invested lines	59	53
Total Line Reinforcement (MW)	546.24	467.92
Avoided Line Reinforcement (MW)	-	72.58
Investment on the NRCC (Million \$)	-	92.10
Total Saved Cost (Million \$)	-	94.32

Taken together, Figs. 6 and 7 show how BESSs funded by the NRCC service shift hours of low marginal transmission loading into the peak periods, flattening the peak magnitude and tightening both the direct and reverse netload envelopes. This operational pattern underlies the transmission investment deferrals reported in the following subsection.

C. Results of NRCC-Informed Transmission System Planning

With NRCCs from the distribution side, we present the NRCC-informed transmission system planning results to demonstrate the benefits of NRCC adoption from the transmission network's perspective. Here, we assume that all substations connected to transmission nodes are capable of providing NRCCs. Fig. 8 presents transmission network maps comparing line reinforcement results for two cases: (a) without NRCC and (b) with NRCC. Table II provides the corresponding quantitative results, highlighting the impact of NRCC adoption on transmission investments.

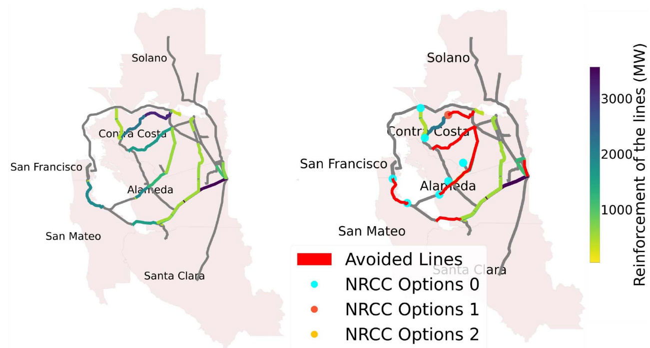

(a) Without NRCC (b) With NRCC

Fig. 8. Map of Line Reinforcement and NRCC Investment in the Bay Area With and Without the NRCC Service.

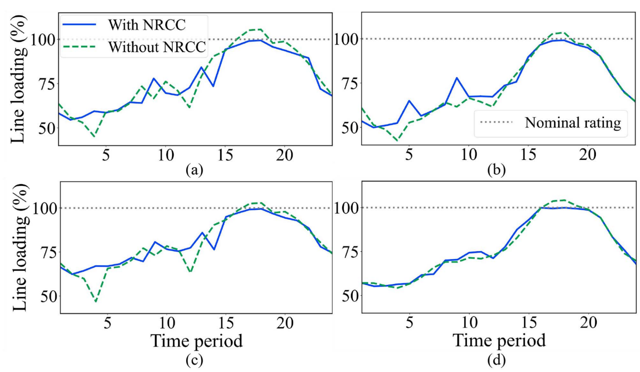

Fig. 9. Normalized line loadings with/without NRCC service on the peak day under the maximum netload scenario on selected lines: (a) Line 43, (b) Line 90, (c) Line 104, and (d) Line 118.

Without NRCC integration, 59 transmission lines require significant reinforcement, with a total capacity of 546.24 MW. With T&D coordination, however, NRCC services are procured at 10 buses, avoiding the reinforcement of 6 transmission lines, as highlighted in red in Fig. 8(b). This corresponds to a total avoided capacity of 72.58 MW, resulting in cost savings of \$186.42 million, i.e., a 16.5% reduction in overall transmission investment costs. Notably, while NRCC adoption requires an additional investment of \$92.10 million paid to DSOs for distribution-level upgrades, these costs are more than offset by savings from reduced transmission investments. The net cost savings amount to \$94.32 million, highlighting the economic efficiency and practicality of the NRCC-integrated framework.

Lastly, Fig. 9 plots the hourly loading of four representative transmission lines, normalized by their thermal ratings, for the peak day under the maximum netload scenario. Without NRCC, these four lines exceed their original capacities during peak hours, necessitating costly reinforcements. In contrast, with NRCC in place, the loadings stay safely below the limits. The difference comes from the extra BESS capacity installed by the DSO: the batteries charge off-peak and discharge at the peak, shaving the substation demand and keeping the line flows within their thermal envelopes. Since thermal limits are satisfied even under the maximum scenarios on the peak day, and no feasibility slack variables are activated, the results also confirm that adopting NRCCs does not compromise system reliability.

V. Conclusion

This paper introduces a novel approach to coordinating T&D planning through the methodology of NRCCs. The proposed NRCC framework addresses critical gaps in current planning processes by explicitly accounting for DER growth uncertainty and integrating long-term flexibility from distribution networks into transmission planning, while not compromising the current regulatory structure. NRCCs achieve this by offering TSOs a "menu" of substation netload guarantees along with corresponding costs, enabling TSO and DSOs to allocate investments more effectively. Key contributions of this work include the development of a TADNP model, an iterative method for computing NRCCs, and the seamless integration of NRCCs into transmission system planning without violating existing regulations. Case studies based on realistic transmission and distribution networks demonstrate that NRCC adoption prevents costly transmission reinforcements while maintaining system operational security and feasibility. Notably, with additional investment budgets from NRCC services procured by the TSO, DSOs can identify investment solutions that incorporate additional BESS installations while reducing the need for local infrastructure upgrades. This underscores the incentives of the NRCC framework in offsetting the high costs of NWAs while supporting resource-efficient planning strategies. Finally, we note that our analysis centers on DSO-owned BESSs as the primary driver of netload reduction. The NRCC framework, however, could be extended to include other DSO assets or third-party resources under different regulatory regimes, which is an area we leave for future work.

Appendix A
Detailed Formulation of NRCC-Informed Transmission Planning Model

This appendix presents our detailed formulation for the NRCC-informed transmission network planning model (3). The model couples long-term transmission-investment decisions with hourly operations under a set of netload scenarios and NRCCs supplied by DSOs. We summarize the formulation here for ease of reference including the necessary extra mathematical symbols in the supplementary nomenclature.

A. Supplementary Nomenclature

Parameters

$\mathrm{cap}^{\dagger}_{ij,h}$	Capacity of conductor option h
$C^{\mathrm{L},\dagger}_{ij,h}$	Annualized investment cost of line option h
$C^{\mathrm{I},\dagger}$	Penalty cost for imbalance
$X^{\dagger}_{ij}$	Reactance of line in DC power flow.
$\overline{P}^{\mathrm{G},\dagger}_{g}$	Capacity limit of generation g
$\overline{R}^{\mathrm{up},\dagger}_{g}/\overline{R}^{\mathrm{dw},\dagger}_{g}$	Percentage of generator g can be used as up/down reserve.
RU_g/RD_g	Percentage of ramp-up/down capability of generator g

$\overline{P}_b^{\mathrm{st,c},\dagger}/\overline{P}_b^{\mathrm{st,d}\dagger}$	Charging/discharging rate limits of storage b
$\eta_b^{\mathrm{c},\dagger}/\eta_b^{\mathrm{d},\dagger}$	Charging/discharging efficiency of storage b

Sets and indices

$\mathcal{H}_{ij}$	Set of conductor options.
$\mathcal{L}^{\mathrm{TN}}$	Set of all transmission corridors.
G_i	Set of generators at bus i
B_i	Set of battery storages at bus i
(i,j)	Index of transmission corridor from i to j
h	Index of conductor options.
g	Index of generator installed on the transmission side.
b	Index of battery storage installed on the transmission side.

Variables

$x_{ij,h}^{\mathrm{L},\dagger}$	Binary variable indicating line reinforcement with the option h
$r_{g,d,t,s}^{\mathrm{up},\dagger}$	Up reserve of generator g
$r_{g,d,t,s}^{\mathrm{dw},\dagger}$	Down reserve of generator g
$\overline{s}_{ij}^{\mathrm{L},\dagger}$	Thermal limit of line (i,j) once $x_{ij,h}^{\mathrm{L}}$ is chosen.
$p_{g,d,t,s}^{G,\dagger}$	Output of generator g
$p_{b,d,t,s}^{\mathrm{st,c},\dagger}/p_{b,d,t,s}^{\mathrm{st,d},\dagger}$	Charging/discharging power of storage unit b
$e_{b,d,t,s}^{\mathrm{st},\dagger}$	State of charge of storage b
$T_b^{\mathrm{st},\dagger}$	Duration of storage b
$p_{i,d,t,s}^{I,+,\dagger}/p_{i,d,t,s}^{I,-,\dagger}$	Upward/downward slack variable at bus i
$p_{ij,d,t,s}^{\mathrm{L},\dagger}$	Power flow on line (i,j)
$\theta_{i,d,t,s}^{\dagger}$	Voltage angle at bus i

B. Mathematical Formulation

$$\begin{aligned}\min &\sum_{(i,j)\in\mathcal{L}^{\mathrm{TN}}}\sum_{h\in\mathcal{H}_{ij}} C_{ij,h}^{\mathrm{L},\dagger}\, x_{ij,h}^{\mathrm{L},\dagger}\mathrm{cap}_{ij,h}^{\dagger}\\ &+\sum_{i\in\mathcal{N}^{\mathrm{TN}}}\sum_{k\in\mathcal{K}}\Delta\Gamma_{i,k}x_{i,k}^{\mathrm{NRCC},\dagger}\\ &+\sum_{i\in\mathcal{N}^{\mathrm{TN}}}\sum_{d\in\mathcal{D}}\sum_{t\in\mathcal{T}}\sum_{s\in\mathcal{S}} w_d\cdot\mathrm{prob}_s\cdot C^{I,\dagger}(p_{i,d,t,s}^{I,+,\dagger}\\ &+p_{i,d,t,s}^{I,-,\dagger})\end{aligned}\tag{A.1}$$

Subject to:

$$\overline{s}_{ij}^{\mathrm{L},\dagger}=\sum_{h\in\mathcal{H}_{ij}} x_{ij,h}^{\mathrm{L},\dagger}\mathrm{cap}_{ij,h}^{\dagger},\ \forall(i,j)\in\mathcal{L}^{\mathrm{TN}}\tag{A.2}$$

$$\sum_{h\in\mathcal{H}_{ij}} x_{ij,h}^{\mathrm{L}}=1,\ \forall(i,j)\in\mathcal{L}^{\mathrm{TN}}\tag{A.3}$$

$$\sum_{k\in\mathcal{K}} x_{i,k}^{\mathrm{NRCC},\dagger}\le 1,\ \forall i\in\mathcal{N}^{\mathrm{TN}}\tag{A.4}$$

$$x_{ij,h}^{\mathrm{L},\dagger}\in\{0,1\},\ \forall(i,j)\in\mathcal{L}^{\mathrm{TN}},h\in\mathcal{H}_{ij}\tag{A.5}$$

$$x_{i,k}^{\mathrm{NRCC},\dagger}\in\{0,1\},\ \forall i\in\mathcal{N}^{\mathrm{TN}},k\in\mathcal{K}\tag{A.6}$$

$$\begin{aligned}&\sum_{g\in G_i} p_{g,d,t,s}^{\mathrm{G},\dagger}+\sum_{b\in\mathcal{B}_i}(p_{b,d,t,s}^{\mathrm{st,d},\dagger}-p_{b,d,t,s}^{\mathrm{st,c},\dagger})-p_{i,d,t,s}^{I,-,\dagger}\\ &\quad+p_{i,d,t,s}^{I,+,\dagger}=D_{i,d,t,s}^{\mathrm{load},\dagger}+\sum_{j|(i,j)\in\mathcal{L}^{\mathrm{TN}}} p_{ij,d,t,s}^{\mathrm{L},\dagger}\\ &\quad-\sum_{j|(j,i)\in\mathcal{L}^{\mathrm{TN}}} p_{ji,d,t,s}^{\mathrm{L},\dagger},\ \forall i\in\mathcal{N}^{\mathrm{TN}},d\in\mathcal{D},t\in\mathcal{T},s\in\mathcal{S}\end{aligned}\tag{A.7}$$

$$p_{i,d,t,s}^{I,+,\dagger}\ge 0,\ \ p_{i,d,t,s}^{I,-,\dagger}\ge 0,\ \forall i\in\mathcal{N}^{\mathrm{TN}},d\in\mathcal{D},t\in\mathcal{T},\ s\in\mathcal{S}\tag{A.8}$$

$$\begin{aligned}&-(1-x_{ij,h}^{\mathrm{L},\dagger})M\le p_{ij,d,t,s}^{\mathrm{L},\dagger}-\frac{1}{X_{ij,h}^{\dagger}}\left(\theta_{i,d,t,s}^{\dagger}-\theta_{j,d,t,s}^{\dagger}\right)\\ &\quad\le(1-x_{ij,h}^{\mathrm{L},\dagger})M,\ \forall(i,j)\in\mathcal{L}^{\mathrm{TN}},d\in\mathcal{D},t\in\mathcal{T},\\ &\qquad h\in\mathcal{H}_{ij},s\in\mathcal{S}\end{aligned}\tag{A.9}$$

$$-\overline{s}_{ij}^{\mathrm{L},\dagger}\ \le\ p_{ij,d,t,s}^{\mathrm{L},\dagger}\ \le\ \overline{s}_{ij}^{\mathrm{L},\dagger},\ \forall(i,j)\in\mathcal{L}^{\mathrm{TN}},\ d\in\mathcal{D},t\in\mathcal{T},s\in\mathcal{S}\tag{A.10}$$

$$r_{g,d,t,s}^{\mathrm{dw},\dagger}\le p_{g,d,t,s}^{\mathrm{G},\dagger}\le\overline{P}_g^{\mathrm{G},\dagger}-r_{g,d,t,s}^{\mathrm{up},\dagger}\ \forall g\in G,\ d\in\mathcal{D},t\in\mathcal{T},s\in\mathcal{S}\tag{A.11}$$

$$0\le r_{g,d,t,s}^{\mathrm{dw},\dagger}\le\overline{P}_g^{\mathrm{G},\dagger}\overline{R}_g^{\mathrm{dw},\dagger},\forall g\in G,d\in\mathcal{D},\ t\in\mathcal{T},s\in\mathcal{S}\tag{A.12}$$

$$0\le r_{g,d,t,s}^{\mathrm{up},\dagger}\le\overline{P}_g^{\mathrm{G},\dagger}\overline{R}_g^{\mathrm{up},\dagger},\forall g\in G,d\in\mathcal{D},\ t\in\mathcal{T},s\in\mathcal{S}\tag{A.13}$$

$$p_{g,d,t,s}^{\mathrm{G},\dagger}-p_{g,d,t-1,s}^{\mathrm{G},\dagger}\le RU_g\overline{P}_g^{\mathrm{G},\dagger},\ \forall g\in G,d\in\mathcal{D},\ t\in\mathcal{T}|t\ge 2,s\in\mathcal{S}\tag{A.14}$$

$$p_{g,d,t-1,s}^{\mathrm{G},\dagger}-p_{g,d,t,s}^{\mathrm{G},\dagger}\le RD_g\overline{P}_g^{\mathrm{G},\dagger},\ \forall g\in G,d\in\mathcal{D},\ t\in\mathcal{T}|t\ge 2,s\in\mathcal{S}\tag{A.15}$$

$$0\le p_{b,d,t,s}^{\mathrm{st,c},\dagger}\le\overline{P}_b^{\mathrm{st,c},\dagger},\forall b\in\mathcal{B},d\in\mathcal{D},t\in T,s\in\mathcal{S}\tag{A.16}$$

$$0\le p_{b,d,t,s}^{\mathrm{st,d},\dagger}\le\overline{P}_b^{\mathrm{st,d}\dagger},\forall b\in\mathcal{B},d\in\mathcal{D},t\in T,s\in\mathcal{S}\tag{A.17}$$

$$d\in\mathcal{D},t\in T,s\in\mathcal{S}\tag{A.18}$$

$$\begin{aligned}e_{b,d,t,s}^{\mathrm{st},\dagger}&=e_{b,d,s}^{\mathrm{st,ini}}+\eta_b^{\mathrm{c},\dagger}p_{b,d,t,s}^{\mathrm{st,c},\dagger}\Delta t\\ &\quad-(1/\eta_b^{\mathrm{d},\dagger})p_{b,d,t,s}^{\mathrm{st,d},\dagger}\Delta t,\forall b\in\mathcal{B},d\in\mathcal{D},\\ &\quad t=t_d^{\mathrm{ini}},s\in\mathcal{S}\end{aligned}\tag{A.19}$$

$$\begin{aligned}e_{b,d,t,s}^{\mathrm{st},\dagger}&=e_{b,d,t-1,s}^{\mathrm{st},\dagger}+\eta_b^{\mathrm{c},\dagger}p_{b,d,t,s}^{\mathrm{st,c},\dagger}\Delta t\\ &\quad-(1/\eta_b^{\mathrm{d},\dagger})p_{b,d,t,s}^{\mathrm{st,d},\dagger}\Delta t,\forall b\in\mathcal{B},d\in\mathcal{D},\\ &\quad t\in\mathcal{T}|t\ne t_d^{\mathrm{ini}},s\in\mathcal{S}\end{aligned}\tag{A.20}$$

$$e_{b,d,t,s}^{\mathrm{st},\dagger}=e_{b,d,s}^{\mathrm{st,ini}},\forall b\in\mathcal{B},d\in\mathcal{D},t=t_d^{\mathrm{last}},s\in\mathcal{S}\tag{A.21}$$

$$0\le e_{b,d,t,s}^{\mathrm{st},\dagger}\le T_b^{\mathrm{st},\dagger}\overline{P}^{\mathrm{st,c},\dagger},\forall b\in\mathcal{B},d\in\mathcal{D},$$

$$d \in \mathcal{D}, t \in \mathcal{T}, s \in \mathcal{S} \quad (A.22)$$

$$D^{\text{load},\dagger}_{i,d,t,s} = D^{\text{load},0}_{i,d,t,s} + \sum_{k \in \mathcal{K}} \left[p^{\text{sub}}_{i,d,t,s}(\Delta\Gamma_{i,k}) - D^{\text{load},0}_{i,d,t,s} \right] x^{\text{NRCC},\dagger}_{i,k}, \ \forall i \in \mathcal{N}^{\text{TN}}, d \in \mathcal{D}, t \in \mathcal{T}, s \in \mathcal{S} \quad (A.23)$$

where objective function (A.1) minimizes the sum of: (i) reinforcement cost of candidate transmission lines, (ii) capital costs of selected NRCC options, and (iii) expected penalty costs for load shedding to maintain feasibility. Constraints (A.2)–(A.3) provide the explicit version of the planning layer (3b). Specifically, (A.2) translates the binary conductor-selection variable into a thermal-limit value, while (A.3) ensures that exactly one conductor type is chosen for every candidate corridor. Note that corridors that are not candidate for investment will only have one capacity option in (A.2)–(A.3) and this option will be associated with zero cost in the objective function (A.1). Keeping an existing line with the same capacity will also have a null cost in (A.1). (A.7)–(A.22) expand the operational layer (3c). The nodal power-balance relation is formulated in (A.7). Non-negativity of the up- and down-slack variables is imposed by (A.8). For clarity and tractability, a DC power-flow approximation is adopted in (A.9), and the resulting line flows are then bounded by the thermal limits in (A.10), which inherit the conductor choice from (A.2). Constraints (A.11)–(A.15) collect the operating constraints for generators, where capacity restrictions, reserve scheduling, and ramping limits are considered. Constraints (A.16)–(A.22) depict the storage operation and limits. Constraints (A.4), (A.6) and (A.23) are NRCC-related constraints which are explained in detail in Section II-D.

Acknowledgment

The authors would like to thank P. Castillo Ibacache (PUC-Chile) and A. Valenzuela (Lawrence Berkeley National Laboratory) for their help with organizing the data for the case study.

References

[1] A. L. Cooke, J. S. Homer, and L. C. Schwartz, "Distribution system planning-state examples by topic," Pacific Northwest Nat. Lab., Richland, WA, USA, Tech. Rep. PNNL-27366, 2018.

[2] Pacific Gas & Electric Company (PG&E), "PG&E's 2021 distribution grid needs assessments," filing to the California Public Utilities Commission, Aug. 16, 2021. [Online]. Available: https://docs.cpuc.ca.gov/PublishedDocs/Efile/G000/M400/K642/400642070.PDF

[3] K. Bell and S. Gill, "Delivering a highly distributed electricity system: Technical, regulatory and policy challenges," *Energy Policy*, vol. 113, pp. 765–777, 2018.

[4] I. Mezghani, N. Stevens, A. Papavasiliou, and D. I. Chatzigiannis, "Hierarchical coordination of transmission and distribution system operations in European balancing markets," *IEEE Trans. Power Syst.*, vol. 38, pp. 3990–4002, Sep. 2023.

[5] S. Choi, "Practical coordination between day-ahead and real-time optimization for economic and stable operation of distribution systems," *IEEE Trans. Power Syst.*, vol. 33, no. 4, pp. 4475–4487, Jul. 2018.

[6] B. Zhang et al., "Transmission and decision-making co-design for active support of region frequency regulation through distribution network-side resources," *IEEE Trans. Circuits Syst., Reg. Papers*, vol. 70, no. 10, pp. 4204–4217, Oct. 2023.

[7] G. Valverde, D. Shchetinin, and G. Hug-Glanzmann, "Coordination of distributed reactive power sources for voltage support of transmission networks," *IEEE Trans. Sustain. Energy*, vol. 10, no. 3, pp. 1544–1553, Jul. 2019.

[8] M. Wang, Y. Wu, M. Yang, M. Wang, and L. Jing, "Dynamic economic dispatch considering transmission–distribution coordination and automatic regulation effect," *IEEE Trans. Ind. Appl.*, vol. 58, no. 3, pp. 3164–3174, May/Jun. 2022.

[9] Electric Power Research Institute (EPRI), "TSO-DSO coordination functions for DER," Palo Alto, CA, USA, Tech. Rep. 3002021985, Jan. 2022.

[10] European Commission, "Large scale campaigns to demonstrate how TSO-DSO shall act in a coordinated manner to procure grid services in the most reliable and efficient way (CoordiNet)," Horizon 2020 Project CoordiNet, Grant Agreement No. 824414, 2019.

[11] T. Kavulla, "Why is the smart grid so dumb? Missing incentives in regulatory policy for an active demand side in the electric sector," Energy Syst. Integr. Group, Reston, VA, USA, White Paper, Jan. 2023. [Online]. Available: https://www.esig.energy/aligning-retail-pricing-with-grid-needs

[12] F. Heymann, J. Silva, V. Miranda, J. Melo, F. J. Soares, and A. Padilha-Feltrin, "Distribution network planning considering technology diffusion dynamics and spatial net-load behavior," *Int. J. Elect. Power Energy Syst.*, vol. 106, pp. 254–265, 2019.

[13] L. Baringo, L. Boffino, and G. Oggioni, "Robust expansion planning of a distribution system with electric vehicles, storage and renewable units," *Appl. Energy*, vol. 265, 2020, Art. no. 114679.

[14] Y. Li, F. Qiu, Y. Chen, and Y. Hou, "Adaptive distributionally robust planning for renewable-powered fast charging stations under decision-dependent EV diffusion uncertainty," *IEEE Trans. Smart Grid*, vol. 15, no. 6, pp. 5853–5870, Nov. 2024.

[15] G. Muñoz-Delgado, J. Contreras, J. M. Arroyo, A. S. de la Nieta, and M. Gibescu, "Integrated transmission and distribution system expansion planning under uncertainty," *IEEE Trans. Smart Grid*, vol. 12, no. 5, pp. 4113–4125, Sep. 2021.

[16] M. Movahednia, R. Mahroo, and A. Kargarian, "Transmission-distribution coordination for enhancing grid resiliency against flood hazards," *IEEE Trans. Power Syst.*, vol. 39, no. 3, pp. 5272–5282, May 2024.

[17] Z. Yuan et al., "Resilience enhancement of coordinated transmission and distribution system via risk-based decentralized planning against typhoons," *IEEE Trans. Ind. Appl.*, vol. 61, no. 4, pp. 5780–5796, Jul./Aug. 2025.

[18] F. Najibi, D. Apostolopoulou, and E. Alonso, "TSO-DSO coordination schemes to facilitate distributed resources integration," *Sustainability*, vol. 13, no. 14, 2021, Art. no. 7832.

[19] K. Nainar, "Hierarchical distributed control of active electric power distribution grids," Ph.D. dissertation, Aalborg Univ., Aalborg, Denmark, 2019.

[20] J. Zhao, H. Wang, Y. Liu, Q. Wu, Z. Wang, and Y. Liu, "Coordinated restoration of transmission and distribution system using decentralized scheme," *IEEE Trans. Power Syst.*, vol. 34, no. 5, pp. 3428–3442, Sep. 2019.

[21] H. Le Cadre, I. Mezghani, and A. Papavasiliou, "A game-theoretic analysis of transmission-distribution system operator coordination," *Eur. J. Oper. Res.*, vol. 274, no. 1, pp. 317–339, 2019.

[22] Electric Power Research Institute (EPRI), "Transmission and distribution operations and planning coordination: TSO/DSO and Tx/Dx planning interaction, processes, and data exchange," Palo Alto, CA, USA, Tech. Rep. 3002016712, 2019.

[23] Y. Chen, Q. Guo, and H. Sun, "Decentralized unit commitment in integrated heat and electricity systems using SDM-GS-ALM," *IEEE Trans. Power Syst.*, vol. 34, no. 3, pp. 2322–2333, May 2019.

[24] Independent Electricity System Operator (IESO), "Regional planning process review: Final report," Toronto, ON, Canada, Feb. 2021. [Online]. Available: https://www.ieso.ca/-/media/Files/IESO/Document-Library/engage/rpr/rprp-20210204-final-report.pdf

[25] J. Silva et al., "Estimating the active and reactive power flexibility area at the TSO-DSO interface," *IEEE Trans. Power Syst.*, vol. 33, no. 5, pp. 4741–4750, Sep. 2018.

[26] F. Capitanescu, "Computing cost curves of active distribution grids aggregated flexibility for TSO-DSO coordination," *IEEE Trans. Power Syst.*, vol. 39, no. 1, pp. 2381–2384, Jan. 2024.

[27] A. Churkin, M. Sanchez-Lopez, M. I. Alizadeh, F. Capitanescu, E. A. M. Ceseña, and P. Mancarella, "Impacts of distribution network reconfiguration on aggregated DER flexibility," in *Proc. IEEE Belgrade PowerTech*, 2023, pp. 1–7.

[28] North American Electric Reliability Corporation (NERC), "2024 summer reliability assessment," Atlanta, GA, USA, Reliability Assessment, May 2024.

[29] California Public Utilities Commission (CPUC), "2024 distributed energy resources avoided cost calculator documentation," Version 1b, Oct. 2, 2024. [Online]. Available: https://www.cpuc.ca.gov/-/media/cpuc-website/divisions/energy-division/documents/demand-side-management/acc-models-latest-version/updated-2024-acc-documentation-v1b.pdf
[30] Pacific Gas and Electric Company (PG&E), "2023 Distribution Grid Needs Assessment Report," San Francisco, CA, USA, Aug. 15, 2023. [Online]. Available: https://www.pge.com/assets/pge/docs/about/doing-business-with-pge/GNA.pdf
[31] National Renewable Energy Laboratory (NREL), "SMART-DS synthetic electrical network data OpenDSS models for SFO, GSO, and AUS," 2020. [Online]. Available: https://data.openei.org/submissions/2981
[32] S. Taylor, A. Rangarajan, N. Rhodes, J. Snodgrass, B. C. Lesieutre, and L. A. Roald, "California test system (CATS): A geographically accurate test system based on the California grid," *IEEE Trans. Energy Markets, Policy Regulation*, vol. 2, no. 1, pp. 107–118, Mar. 2024.
[33] W. H. Kersting, "Distribution system modeling and analysis," in *Electric Power Generation, Transmission, and Distribution*. Boca Raton, FL, USA: CRC Press, 2018, pp. 26–1.
[34] National Renewable Energy Laboratory (NREL), "Distribution system upgrade unit cost database current version," 2019. [Online]. Available: https://data.nrel.gov/submissions/101
[35] National Renewable Energy Laboratory (NREL), "The regional energy deployment system (ReEDS)," 2024. [Online]. Available: https://github.com/NREL/ReEDS-2.0
[36] Y. Li, S. Córdova, A. Moreira, and M. Heleno, "Dataset for netload range cost curves for coordinated transmission-distribution planning under der growth uncertainty," *IEEE Dataport*, 2025, doi: 10.21227/grcg-9058.
[37] National Renewable Energy Laboratory (NREL), "Cambium datasets," 2024. [Online]. Available: https://www.nrel.gov/analysis/cambium.html
[38] B. Sigrin, M. Gleason, R. Preus, I. Baring-Gould, and R. Margolis, "Distributed generation market demand model (DGEN): Documentation," Nat. Renew. Energy Lab. (NREL), Golden, CO, USA, Tech. Rep. NREL/TP-6A20-65231, 2016.
[39] E. Kiesling, M. Günther, C. Stummer, and L. M. Wakolbinger, "Agent-based simulation of innovation diffusion: A review," *Central Eur. J. Operations Res.*, vol. 20, pp. 183–230, 2012.
[40] F. Murtagh and P. Contreras, "Algorithms for hierarchical clustering: An overview," *Wiley Interdiscipl. Rev., Data Mining Knowl. Discov.*, vol. 2, no. 1, pp. 86–97, 2012.
[41] K. Poncelet, H. Höschle, E. Delarue, A. Virag, and W. D'haeseleer, "Selecting representative days for capturing the implications of integrating intermittent renewables in generation expansion planning problems," *IEEE Trans. Power Syst.*, vol. 32, no. 3, pp. 1936–1948, May 2017.

Yujia Li (Member, IEEE) received the B.E. degree in electrical engineering and automation from the Huazhong University of Science and Technology, Wuhan, China, in 2018, and the Ph.D. degree in electrical and electronic engineering from The University of Hong Kong, Hong Kong, in 2022. She was a Postdoctoral Researcher with The University of Hong Kong, from 2022 to 2024. She is currently a Postdoctoral Researcher with Lawrence Berkeley National Laboratory, Berkeley, CA, USA. Her research interests include power system resilience, transportation electrification, and uncertainty quantification.

Samuel Córdova (Member, IEEE) received the M.Sc. degree in electrical engineering from the Pontificia Universidad Católica de Chile (PUC-Chile), Santiago, Chile, in 2017, and the Ph.D. degree in electrical and computer engineering from the University of Waterloo, Waterloo, ON, Canada, in 2023. In 2023, he was a Postdoc Scholar with Grid Integration Group, Lawrence Berkeley National Laboratory, Berkeley, CA, USA. He is currently an Assistant Professor with the Department of Electrical Engineering and Member of UC Energy Research Center, PUC-Chile. His research focuses on the operation, control, and optimization of modern power systems with a large integration of renewable and inverter-based resources.

Alexandre Moreira (Senior Member, IEEE) received the Electrical Engineering and Industrial Engineering degrees from the Pontifical Catholic University of Rio de Janeiro (PUC-Rio), Rio de Janeiro, Brazil, in 2011, the M.Sc. degree from the Electrical Engineering Department, PUC-Rio, in 2014, and the Ph.D. degree from the Department of Electrical and Electronic Engineering, Imperial College London, London, U.K., in 2019. He is currently a Research Scientist with Lawrence Berkeley National Laboratory, Berkeley, CA, USA. His research interests include decision-making under uncertainty and power system economics, operation, and planning.

Miguel Heleno (Senior Member, IEEE) received the M.Sc. degree in electrical engineering and computer science and the Ph.D. degree in sustainable energy systems within the MIT Portugal Program from the University of Porto, Porto, Portugal. He is currently a Staff Scientist with Lawrence Berkeley National Laboratory, Berkeley, CA, USA. His research interests include power systems planning and economics.